Advances in Continuous and Discrete Models

RESEARCH Open Access

Mathematical modelling of the transmission dynamics of Marburg virus disease with optimal control and cost-effectiveness analysis based on lessons from Ebola virus disease

John Amoah-Mensah[1*], Nicholas Kwasi-Do Ohene Opoku[2,4*], Reindorf Nartey Borkor[2], Francis Ohene Boateng[3], Kwame Bonsu[1], Vida Afosaa[1] and Rhoda Afutu[1]

*Correspondence:
amoahmensahjohn@gmail.com;
nicholas@aims.edu.gh
[1]Department of Computer Science, Sunyani Technical University, Sunyani, Ghana
[2]Kwame Nkrumah University of Science and Technology, Kumasi, Ghana
Full list of author information is available at the end of the article

Abstract

Marburg virus, like Ebola, causes haemorrhagic disease with high fatality rates. We developed a deterministic SEIRDVT model incorporating vaccination and treatment to study the disease dynamics. Qualitative analysis revealed a backward bifurcation when $R_0 = 1$, meaning $R_0 < 1$ is insufficient to eradicate the virus. Sensitivity analysis using Latin Hypercube Sampling showed that applying four control measures—screening, prevention, continuous vaccination, and treatment—significantly reduced transmission. The most cost-effective strategy combines prevention, vaccination, and treatment. These findings provide a framework for designing efficient interventions to combat Marburg virus.

Keywords: Filovirdae; Epidemiology; Marburg virus disease; Optimal control strategies; Disease transmission; Basic reproduction number; Sensitivity analysis; Cost-effectiveness analysis

1 Introduction

The Marburg virus disease (MVD) was discovered in 1967. Like Ebola, MVD belongs to the deadly Filovirus family of viruses and is transmitted among people and non-human primates [1]. MVD is characterized by an acute haemorrhagic fever with a fatality ratio of up to 88% [1]. It affects humans when an individual comes into contact with contaminated blood or the bodily fluids of an infected person. The worst MVD outbreak recorded occurred between 2004 and 2005 in Uige, Angola, with 252 people infected and about 90% of them died. Afterwards, several cases of MVD have been reported across the globe. For example, MVD was recorded in Kween district of eastern Uganda (2017), Guinea (2021), and Ashanti region of Ghana (2022) [2].

Similar to Ebola, the manifestation of Marburg symptoms often occurs within a range of 2 to 21 days. It is worth noting that for Ebola, the average incubation period is reported to be approximately 8 to 10 days. The symptoms associated with Marburg infection may encompass the abrupt onset of fever, chills, headache, bodily discomfort, as well as the development of a rash over the chest, back, and abdomen [3]. In instances of heightened severity, those who have contracted the infection may experience symptoms such as nausea, vomiting, chest discomfort, sore throat, abdominal pain, or diarrhea, and in extreme cases, mortality may occur [3]. However, unlike Ebola, there are presently no medically approved vaccines or medicines to treat MVD, but the 2013 – 2016 Ebola virus resurgence and current pandemic in West Africa brought to light the tremendous threat filovirus epidemics represent to global public health. Therefore, despite the successful containment of previous outbreaks of MVD without the use of essential interventions such as vaccination or comprehensive treatment, there is the need to develop new and effective strategies to address potential future large-scale outbreaks in situations where the implementation of public health measures is not feasible or fails. Due to the significant severity and fatality associated with MVD, along with other filoviruses such as Ebola virus, the reemergence of MVD would pose a substantial risk to human health. This risk is particularly pronounced in situations where vaccination, treatment, and other preventive measures are unavailable.

The utilization of mathematical models enables researchers and policymakers to ascertain the optimal approaches for combating infectious diseases. These models can be used to examine hypothetical scenarios, both at the national and regional levels, with the aim of enhancing public health outcomes and minimizing financial burdens. Although there exist various strategies for preventing infectious diseases and conducting scientific research on diseases, mathematical modeling offers a rational and evidence-driven framework for addressing these concerns and resolving the issue in an optimal and systematic manner. For example, [4] evaluated the transmissibility and severity of the Marburg virus by looking at the largest known Marburg hemorrhagic fever outbreak, which struck Angola in 2005 and resulted in more than 200 deaths. The study by [4] also provided information about the evolution of the viral load of Marburg disease in non-human primates. The authors did not only offered insights into the avoidance of future Marburg hemorrhagic fever epidemics, but also gave valuable guidance for implementing appropriate medical interventions. For example, they determined the fundamental reproduction number to be 1.59 (95% CI: 1.53 – 1.66), while the distribution of the generation time was found to have a mean of 9 days (95% CI: 8.2 – 10 days) and a standard deviation of 5.4 days (95% CI: 3.9 – 8.6 days). Based on the model proposed by [4], they suggested that a prompt isolation of individuals with the onset of symptoms, ideally within a time frame of 2 – 3 days, is sufficient to effectively halt the progression of an MVD outbreak.

In another development [5], two different models were formulated: a small-world network model and a compartmental Susceptible-Exposed-Infectious-Recovered (SEIR) model, to simulate the transmission of MVD. The model by [5] indicated that community participation is vital to successfully reduce MVD epidemics. As stated by the World Health Organization (WHO), an effective outbreak control requires a combination of measures, such as those devoted to infection prevention and control, surveillance, contact tracing, and social mobilization. Recently, a branching process model of Marburg virus transmission was developed by [6]. The study focused on analyzing the potential outcomes of different preventive and reactive vaccination regimens in situations primarily influenced by

multiple spillover events and human-to-human transmission. In contrast to previously reported high case fatality ratio mentioned in [4], the data utilized in [6] indicates a low basic reproduction number of 0.81 (95% CI: 008 – 183). In [6], it was further observed that in the event of an outbreak caused by zoonotic spillovers, initiating the vaccination campaign after the first case has occurred can be effective. By implementing a combination of ring and targeted vaccination strategies, specifically focusing on high-risk groups, there is a 95% confidence interval (CI) indicating the potential to control outbreaks with a success rate of 0.88 (0.60 – 0.91). This is in comparison to a success rate of 0.65 (0.60 – 0.69) if no vaccination is administered.

Another study [7] assessed the dynamics of Marburg virus transmission that incorporates the impact of public health education. Their model incorporated the Caputo fractional-order derivative to extend the traditional integer model to a fractional-based model. Numerical simulations from the model showcase a variety of realistic parameter values that support the argument that human awareness, as a form of education, considerably lowers susceptibility and the risk of infection. However, although the authors added a hospitalization compartment to their model, they failed to assess the effect of treatment on these class of individuals. This observation was in line with the recommendation made by the study [8]. The model in [8] ascertain the effect of contact tracing and quarantine strategies in curtailing the spread of Marburg virus and observed that enhanced contact tracking and efficient quarantine strategies can reduce or stop the spread of the virus. However, the secondary findings from the study revealed that to reduce the number of fatalities caused by infectious cases, treatment therapy must be used. Hence, "if no treatment therapy is used, no infected person will survive the MVD".

The results of these previous studies align with the prevailing notion that infectious diseases with limited ability to spread and severe symptoms are the most manageable in terms of introducing various control measures. However, the lack of compartmental mathematical models on MVD transmission dynamics are worrying, because although the MVD disease is rare, it has the potential to cause dramatic outbreaks with high fatality. Moreover, the constant reoccurrence of the Ebola virus disease, which share the same genus family with MVD, makes the idea of developing enough models similar to those of EBOLA for MVD transmission a necessity. Furthermore, it is worrying to know that there is currently no specific treatment or vaccine for MVD and no model has been developed incorporating these two classes to see the potential cost benefits these models can enlighten or provide the scientific world. Motivated by this situation, the current article, develop a novel MVD mathematical model to ascertain how incorporating both vaccination and treatment as a compartment as well as screening and prevention as control measures can help prevent current and possible future MVD outbreaks. The current model moves a step further to determine the associated cost involved in implementing these controls.

2 Model formulation

We develop a novel MVD model where the host population, $N(t)$, is divided into seven compartments, $S(t)$, $V(t)$, $E(t)$, $I(t)$, $T(t)$, $D(t)$, and $R(t)$. The compartment $S(t)$ denotes the number of susceptible individuals at time t, while $V(t)$, $E(t)$, $I(t)$, $T(t)$, $D(t)$, and $R(t)$, respectively, denote the number of vaccinated, exposed, infected, treated, deceased and recovered individuals at time t. The transition from one compartment to another is shown in Fig. 1 and described in Equation (2).

Equation (2) shows that the population is replenished by a constant recruitment rate λ. But a proportion ρ of these recruited individuals are assumed to receive onset vaccination, while the remaining fraction, $1-\rho$, representing all uninfected individuals who are not protected by vaccination, remain in the susceptible compartment. The model further assumed that future circumstances either by community education or engagement and government policies will cause individuals to be vaccinated at the rate ξ causing them to move from susceptible to the vaccinated compartment. According to the model, it is important to note that only individuals who are currently in compartments I and D are considered to be infectious. In the realm of public health, it is crucial to understand the dynamics of disease transmission. Hence, with MVD, individuals become vulnerable to infection through contact with both susceptible and infectious individuals. This interaction leads to the emergence of new infections, which occur at a rate known as ΨS. Additionally, there is another mode of transmission involving vaccinated individuals who wane their vaccine by coming into contact with infectious individuals, resulting in an incidence rate denoted as ΨV. These factors play a significant role in the spread and impact of MVD within a population. The force of infection, a crucial measure in epidemiology, can be defined as follows:

$$\Psi = \frac{\beta(I+\delta D)}{N}. \tag{1}$$

The other parameters in Equation (2) are as follows: the parameter σ represent exposed individuals transition into the infected compartment. Based on data provided by the World Health Organization (WHO), it has been observed that the average case fatality rate for MVD stands at approximately 50%. Furthermore, historical outbreaks have demonstrated a range of mortality rates spanning from 24% to 88%, with variations attributed to factors such as the specific strain of the virus and the manner in which cases were managed. Thus, the parameter η denotes individuals that die as a result of MVD. The Center for Disease Control and Prevention (CDC), in agreement with WHO, explain that early supportive care with re-hydration, and symptomatic treatment improves survival, hence the parameter α is used to represent individuals that receives treatment, while θ and ω denote infected and treated individual's recovery rates, respectively. The per capita natural death rates for susceptible, vaccinated, exposed, infected, treated and recovered individuals are represented as μS, μV, μE, μI, μT and μR, respectively.

The biological descriptions given in Fig. 1 resulted in the following system of nonlinear differential equations:

$$\begin{aligned}
\frac{dS}{dt} &= (1-\rho)\lambda - (\mu+\Psi+\xi)S,\\
\frac{dV}{dt} &= \lambda\rho + \xi S - (\mu+\Psi)V,\\
\frac{dE}{dt} &= \Psi S + \Psi V - (\mu+\sigma)E,\\
\frac{dI}{dt} &= \sigma E - (\alpha+\theta+\eta+\mu)I,\\
\frac{dT}{dt} &= \alpha I - (\omega+\mu)T,\\
\frac{dR}{dt} &= \theta I + \omega T - \mu R,
\end{aligned} \tag{2}$$

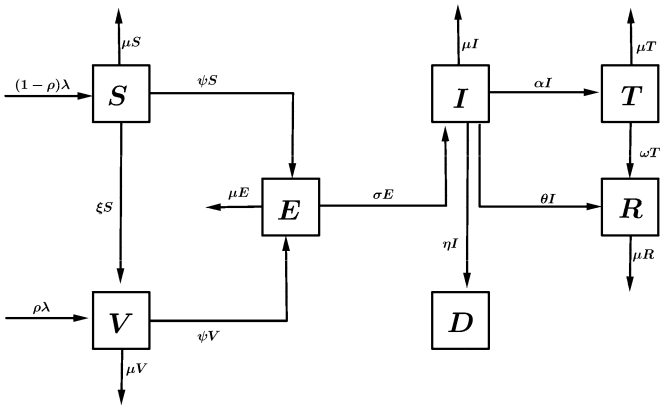

Figure 1 Depicts the sequential stages individuals go through during an epidemic of Marburg virus disease (MVD), and it also illustrates the rates at which people transition from one stage to another

$$\frac{dD}{dt} = \eta I.$$

3 System analysis

3.1 Basic properties

In order to establish the epidemiological significance of system (2), we demonstrate the nonnegativity and boundedness of all state variables at all points in time, as supported by the following theorem:

Theorem 1 *The solutions of system* (2) *are always positive if and only if the initial conditions* $(S(0), V(0), E(0), I(0), T(0), \text{and } R(0))$ *are nonnegative.*

Nonnegative solution: Suppose $S(0) \geq 0$, then from the first equation of system (2), we have:

$$\frac{dS}{dt} = (1-\rho)\lambda - (\mu + \Psi + \xi)S. \tag{3}$$

Since $(1-\rho)$ depicts the recruitment of individuals into the susceptible compartment, it is nonnegative for all $t > 0$. Thus, Equation (3) becomes

$$\begin{aligned}
\frac{dS}{dt} &\geq -(\mu + \Psi + \xi)S, \\
\frac{dS}{S} &\geq -(\mu + \Psi + \xi)dt, \\
\int_0^t \frac{dS}{S} &\geq -\int_0^t (\mu + \Psi + \xi)dt, \\
\ln\left(\frac{S(t)}{S(0)}\right) &\geq -(\mu + \xi)t - \int_0^t \Psi dt, \\
S(t) &\geq S(0)e^{-(\mu+\xi)-\int_0^t \Psi dt} > 0.
\end{aligned}$$

Using the same justifications, we obtain the following results:

$$V(t) \geq V(0)e^{-(\mu t + \int_0^t \Psi dt)} \geq 0,$$

$$E(t) \geq E(0)e^{-(\mu+\sigma)t} > 0,$$

$$I(t) \geq I(0)e^{-(\alpha+\theta+\eta_1+\mu)t} > 0,$$

$$T(t) \geq T(0)e^{-(\omega+\mu)t} > 0,$$

$$R(t) \geq R(0)e^{-\mu t} > 0.$$

Therefore, $S(t), V(t) > 0$ and $E(t), I(t), T(t), R(t) \geq 0$, for all $t > 0$, given the initial conditions. □

Theorem 2 (Boundedness) *The biologically feasible region*, Γ, *is given by the following set*:

$$\Gamma = \left\{(S, V, E, I, T, R, D) \in \mathbb{R}_+^7 : S + V + E + I + T + R + D; N \leq \frac{\lambda}{\mu}\right\},$$

such that for any $t > 0$, *it is positively invariant, attracts system* (2), *and has a finite upper bound*.

Proof We calculate the sum of system (2), which contributes to the rate of change of N over time as $\frac{dN}{dt}$.

$$\frac{dN}{dt} = \lambda - \mu N. \tag{4}$$

Solving Equation (4) produces;

$$N(t) = \frac{\lambda}{\mu} + Ce^{-\mu t}. \tag{5}$$

The traits of Equation (5) is such that

$$0 \leq N(t) \leq N(0)e^{-\mu t} + \frac{\lambda}{\mu}(1 - e^{\mu t}).$$

Therefore, the feasible region Γ is positively invariant and attracting with respect to system (2). □

3.2 Marburg-free equilibrium (MFE)

MFE is the steady-state solution, where MVD is absent in the population. It is easy to check that system (2) has a MFE, $\mathcal{E}^{\#} = (S^{\#}, V^{\#}, 0, 0, 0, 0, 0)$, by setting the right-hand side of system (2) to zero. This yields:

$$\mathcal{E}^{\#} = \left(\frac{\lambda(1-\rho)}{(\mu+\xi)}, \frac{\lambda(\xi+\mu\rho)}{\mu(\mu+\xi)}, 0, 0, 0, 0, 0\right). \tag{6}$$

3.2.1 Basic reproduction number

The basic reproduction number is a key quantity in classical epidemiological models. It is denoted by $\mathcal{R}_0$. It is useful for both predicting disease outbreaks and assessing disease prevention measures. The basic reproduction number can be defined in this context as the expected number of secondary cases, produced by one MVD infectious individual in a totally

susceptible or Marburg-free population. To compute the R_0 of system (2), we use the next-generation method applied in [9]. Hence, from system (2), we derived $\mathcal{F} = (\Psi S + \Psi V, 0, 0)^T$ and $\mathcal{V} = ((\mu+\sigma)E, -\sigma E + (\mu+\eta+\theta+\alpha)I, -\alpha I + (\omega+\mu)T)^T$ to respectively represent the vector of newly generated infections and transfer of infections between compartments, respectively. Thus, the basic reproduction number, which is the spectral radius of FV^{-1} obtained as:

$$\mathcal{R}_0 = \frac{\beta\mu\sigma(1-\rho)}{(\mu+\xi)(\mu+\sigma)(\alpha+\eta+\mu+\theta)}. \tag{7}$$

3.2.2 Stability analysis of MFE

The stability analysis of the MFE point, $\mathcal{E}^{\#}$, is investigated in this section using the following theorem.

Theorem 3 *The Marburg-free equilibrium, $\mathcal{E}^{\#}$, is locally asymptotically stable when $\mathcal{R}_0 < 1$ and unstable otherwise.*

Proof Before evaluating the stability analysis of the MFE, we observed that the last differential equation of system (2) is uncoupled from the other equations and when $\lim_{t\to\infty} I(t) = 0$. Hence, we can solve $\frac{dD}{dt}$ using the integration method to obtain it analytic solution. This gives

$$D(t) = D(0) + \eta \int_0^t I dt.$$

Therefore, the local stability of system (2) can be derived from the first six coupled equations of system (2). This implies obtaining the Jacobian matrix, which is

$$J_{\mathcal{E}^{\#}} = \begin{bmatrix} -(\mu+\xi) & 0 & 0 & \frac{\beta\mu(1-\rho)}{\mu+\xi} & 0 & 0 \\ \xi & -\mu & 0 & -\frac{\beta(\xi+\rho\mu)}{(\mu+\xi)} & 0 & 0 \\ 0 & 0 & -(\sigma+\mu) & 0 & 0 & 0 \\ 0 & 0 & \sigma & -(\alpha+\theta+\eta+\mu) & 0 & 0 \\ 0 & 0 & 0 & \alpha & -(\omega+\mu) & 0 \\ 0 & 0 & 0 & 0 & \omega & -\mu \end{bmatrix}. \tag{8}$$

To achieve local stability, it is necessary (but not sufficient) for the trace of Equation (8) to be negative, but also for the determinant to be positive. Hence, it can be observed that the trace of Equation (8) is negative. By applying row reduction technique, $J_{\xi^{\#}}$, can be reduced to

$$J_{\xi_1^{\#}} = \begin{bmatrix} -(\mu+\xi) & \frac{\beta\mu(1-\rho)}{\mu+\xi} \\ 0 & -(\alpha+\theta+\eta+\mu) \end{bmatrix}. \tag{9}$$

The $\det(J_{\xi_1^{\#}}) > 0$, which completes the proof. Thus, the MFE state is locally stable for $R_0 < 1$. Next, we ascertain the global stability. □

3.2.3 Global stability of MFE

The global stability of MFE is established by applying the method in [10]. Therefore, we rewrite the equations in system (2) as

$$\frac{dX}{dt} = A(X, Y), \tag{10}$$

$$\frac{dY}{dt} = B(X, Y), \qquad B(X, 0) = 0, \tag{11}$$

where $X \in \mathbb{R}^3 = (S, V, R)$ represents the number of uninfected individuals, while $Y \in \mathbb{R}^4$ represent the infected category. Based on the study in [10], the necessary condition to achieve the global stability is given by:

$$\begin{aligned} &\text{Condition 1:} \quad \frac{dX}{dt} = A(X, 0), \quad X^* \text{ is globally asymptotically stable,} \\ &\text{Condition 2:} \quad B(X, Y) = ZY - \hat{B}(X, Y) \geq 0 \quad \text{for} \quad (X, Y) \in \Gamma, \end{aligned} \tag{12}$$

where $Z = \Gamma_Y B(X, 0)$ is an M-matrix, that is the of-diagonal entries of Z are positive and Γ is the region, where system (2) makes epidemiological meaningful. If conditions 1 and 2 are met using system (2), then the following theorem holds.

Theorem 4 *The MFE is globally stable if* $\mathcal{R}_0 < 1$ *and condition* 2 *of Equation* (12) *is satisfied.*

Proof Implementing Equations (11) and (12), we obtain

$$\hat{B}(X, Y) = (B - T)X - \frac{dX}{dt}, \quad \text{where} \quad (B - T) = Z. \tag{13}$$

Equation (13) implies that

$$\frac{dX}{dt} = A(X, 0) = \begin{bmatrix} (1 - \rho)\lambda - (\mu + \xi)S \\ \xi S + \lambda\rho - \mu V \\ 0 \end{bmatrix},$$

$$\frac{dY}{dt} = \begin{bmatrix} \Psi S + \Psi V - (\mu + \sigma)E \\ \sigma E - (\alpha + \mu + \theta + \eta)I \\ \alpha I - (\omega + \mu)T \\ \eta I \end{bmatrix}.$$

Thus,

$$Z = \begin{bmatrix} -(\mu + \sigma) & \dfrac{\beta\mu(1 - \rho)}{\mu + \xi} + \dfrac{\beta(\xi + \rho\mu)}{(\mu + \xi)} & 0 \\ \sigma & -(\mu + \theta + \eta + \alpha) & 0 \\ 0 & \alpha & -(\omega + \mu) \end{bmatrix}, \tag{14}$$

$$\hat{B}(X,Y) = \begin{bmatrix} \beta I\left(\dfrac{\mu(1-\rho)}{\mu+\xi} - \dfrac{S}{N}\right) \\ \beta I\left(\dfrac{(\xi+\mu\rho)}{(\mu+\xi)} - \dfrac{V}{N}\right) \\ 0 \end{bmatrix}. \tag{15}$$

We observe that Equation (14) is stable since the trace is less than zero and determinant greater than zero, which satisfies condition 1, while $S^{\#} > S$ and $V^{\#} > V$, as observed in Equation (15), shows that $\hat{B}(X,Y) > 0$ satisfying condition 2. Thus, it suffice to say that Equation (14) is stable for $R_0 < 1$. Hence, the MFE is globally asymptotically stable for $R_0 < 1$. □

3.3 Marburg-persistent steady states

The Marburg-persistent steady states, $\mathcal{E}^{\star} = S^{\star}, V^{\star}, E^{\star}, I^{\star}, T^{\star}$ and $R^{\star}$, are derived by equating the right-hand terms of the system (2) to zero. Expressing all the variables in terms of the force of infection, Ψ, we get:

$$\begin{aligned}
S^{\star} &= \frac{\lambda(1-\rho)}{\mu+\xi+\Psi^{\star}}, \\
V^{\star} &= \frac{\lambda(\xi+\rho(\mu+\Psi^{\star}))}{(\mu+\Psi^{\star})(\mu+\xi+\Psi^{\star})}, \\
E^{\star} &= \frac{\lambda\Psi^{\star}(1-\rho)}{(\mu+\sigma)(\mu+\xi+\Psi^{\star})}, \\
I^{\star} &= \frac{\lambda\sigma\Psi^{\star}(1-\rho)}{(\alpha+\eta+\theta+\mu)(\mu+\sigma)(\mu+\xi+\Psi^{\star})}, \\
T^{\star} &= \frac{\lambda\alpha\sigma\Psi^{\star}(1-\rho)}{(\alpha+\eta+\theta+\mu)(\mu+\sigma)(\mu+\xi+\Psi^{\star})(\mu+\omega)}, \\
R^{\star} &= \frac{\lambda\sigma\Psi^{\star}(1-\rho)(\alpha\omega+\theta(\mu+\omega))}{\mu(\alpha+\eta+\theta+\mu)(\mu+\sigma)(\mu+\xi+\Psi^{\star})(\mu+\omega)}.
\end{aligned} \tag{16}$$

3.3.1 Local stability of Marburg-persistent steady states

Theorem 5 *The Marburg-persistent steady state* (*MPSS*), *which is defined by* $\mathcal{E}^{\star}$, *is locally asymptotically stable if* $\mathcal{R}_0 > 1$ *and it becomes unstable if* $\mathcal{R}_0 \leq 1$.

Proof We prove the MPSS using the approach in [11, 12]. Based on the solution of Equation (16), we substitute I^{*} for $D = 0$ into Equation (1) and by performing some algebraic manipulation and simplification, we obtain Equation (17):

$$\Upsilon_1\Psi + \Upsilon_0 = 0, \tag{17}$$

where

$$\begin{aligned}
\Upsilon_1 &= (\alpha+\eta+\theta+\mu)(\mu+\sigma), \\
\Upsilon_0 &= (\alpha+\eta+\mu+\theta)(\mu+\sigma)(\mu+\xi) - \beta\sigma\mu(1-\rho) \\
&= (\alpha+\eta+\mu+\theta)(\mu+\sigma)(\mu+\xi)[1-R_0].
\end{aligned} \tag{18}$$

Equation (18) shows that for $R_0 > 1$, the endemic states is unstable while for $R_0 \leq 1$, the system is stable endemically, which calls for further analysis. Hence, in the next section, we performed the bifurcation analysis (see [13]). □

3.4 Existence of bifurcation

Bifurcation refers to a qualitative variation in a system's solution. The bifurcations of the solutions in the neighborhood of the equilibrium points is covered in this section. According to [13], for $R_0 < 1$, disease can be eradicated from the population. But system (2) may exhibit the phenomenon of a backward bifurcation. Because there exists a bi-stability of equilibrium points (one stable disease-free equilibrium and stable endemic equilibrium) for $R_0 < 1$. Epidemiologically, the backward bifurcation is most important, because in this case the system generates another stable endemic equilibrium point for $R_0 < 1$ [14]. This is clearly shown in Equation (18). If a system undergoes a backward bifurcation, we cannot conclude about eradication of disease for $R_0 < 1$. Therefore, for $R_0 < 1$, eradication of disease depends on initial infected population.

We applied the method from [10] such that the bifurcation parameter

$$\beta^+ = \frac{(\alpha+\eta+\theta+\mu)(\mu+\xi)(\mu+\sigma)}{\mu\sigma(1-\rho)},$$

for which $R_0(\beta^+) = 1$. Following [10], the right eigenvector, $(w = (w_1, w_2, w_3, w_4, w_5, w_6)^T)$, associated with the zero eigenvalue represented is obtained as,

$$\begin{pmatrix} -(\mu+\xi) & 0 & 0 & \frac{(\alpha+\eta+\theta+\mu)(\mu+\sigma)}{\sigma} & 0 & 0 \\ 0 & -\mu & 0 & -\frac{(\alpha+\eta+\theta+\mu)(\xi+\mu\rho)(\mu+\sigma)}{\mu(1-\rho)\sigma} & 0 & 0 \\ 0 & 0 & -\mu-\sigma & 0 & 0 & 0 \\ 0 & 0 & \sigma & -\alpha-\eta\theta-\mu & 0 & 0 \\ 0 & 0 & 0 & \alpha & -\mu-\omega & 0 \\ 0 & 0 & 0 & 0 & \omega & -\mu \end{pmatrix} \cdot \begin{pmatrix} w_1 \\ w_2 \\ w_3 \\ w_4 \\ w_5 \\ w_6 \end{pmatrix}, \tag{19}$$

solving for $(w_1, w_2, w_3, w_4, w_5, w_6)$, we obtained the following results:

$$w_1 = \frac{\mu+\sigma}{\mu+\xi}, \quad w_2 = \frac{(\xi+\mu\rho)(\mu+\sigma)}{\mu^2(1-\rho)}, \quad w_3 = 1, \quad w_4 = \frac{\sigma}{\alpha+\eta+\theta+\mu},$$
$$w_5 = \frac{\alpha\sigma}{(\alpha+\eta+\theta+\mu)(\mu+\omega)}, \quad w_6 = \frac{\alpha\sigma\omega}{\mu(\alpha+\eta+\theta+\mu)(\mu+\omega)}.$$

The left eigenvector, $v = (v_1, v_2, v_3, v_4, v_5, v_6)^T$, associated to the zero eigenvalue is obtained as

$$\begin{pmatrix} v_1 & v_2 & v_3 & v_4 & v_5 & v_6 \\ 0 & 0 & 0 & 0 & 0 & 0 \\ 0 & 0 & 0 & 0 & 0 & 0 \\ 0 & 0 & 0 & 0 & 0 & 0 \\ 0 & 0 & 0 & 0 & 0 & 0 \\ 0 & 0 & 0 & 0 & 0 & 0 \end{pmatrix}$$

$$\cdot \begin{pmatrix} -(\mu+\xi) & 0 & 0 & \frac{(\alpha+\eta+\theta+\mu)(\mu+\sigma)}{\sigma} & 0 & 0 \\ 0 & -\mu & 0 & -\frac{(\alpha+\eta+\theta+\mu)(\xi+\mu\rho)(\mu+\sigma)}{\mu(1-\rho)\sigma} & 0 & 0 \\ 0 & 0 & -\mu-\sigma & 0 & 0 & 0 \\ 0 & 0 & \sigma & -\alpha-\eta\theta-\mu & 0 & 0 \\ 0 & 0 & 0 & \alpha & -\mu-\omega & 0 \\ 0 & 0 & 0 & 0 & \omega & -\mu \end{pmatrix}.$$

Solving for $(v_1, v_2, v_3, v_4, v_5, v_6)$, we obtained the following results:

$$v_1 = 1, \quad v_2 = 0, \quad v_3 = 1, \quad v_4 = \frac{\mu+\sigma}{\sigma}, \quad v_5 = 0, \quad v_6 = 0.$$

Thus, the coefficients a and b defined in Theorem 4.1 in [10] are

$$a = \sum_{k,i,j=1}^{n} v_k w_i w_j \frac{\partial^2 f_k}{\partial x_i \partial x_j}(0,0), \tag{20}$$

$$b = \sum_{k,i=1}^{n} w_k w_i \frac{\partial^2 f_k}{\partial x_i \partial \beta^{\#}}(0,0). \tag{21}$$

To solve for a and b, system (2) becomes:

$$\begin{aligned} \frac{dS}{dt} &= (1-\rho)\lambda - (\mu+\Psi+\xi)S = f_1, \\ \frac{dV}{dt} &= \lambda\rho + \xi S - (\mu+\Psi)V = f_2, \\ \frac{dE}{dt} &= \Psi S + \Psi V - (\mu+\sigma)E = f_3, \\ \frac{dI}{dt} &= \sigma E - (\alpha+\theta+\eta+\mu)I = f_4, \\ \frac{dT}{dt} &= \alpha I - (\omega+\mu)T = f_5, \\ \frac{dR}{dt} &= \theta I + \omega T - \mu R = f_6. \end{aligned} \tag{22}$$

Since $v_2 = v_5 = v_6 = 0$, it implies that the second derivatives of f_2, f_5 and f_6 does not have an influence. Hence, following [15], we compute for a and b, the corresponding non-zero

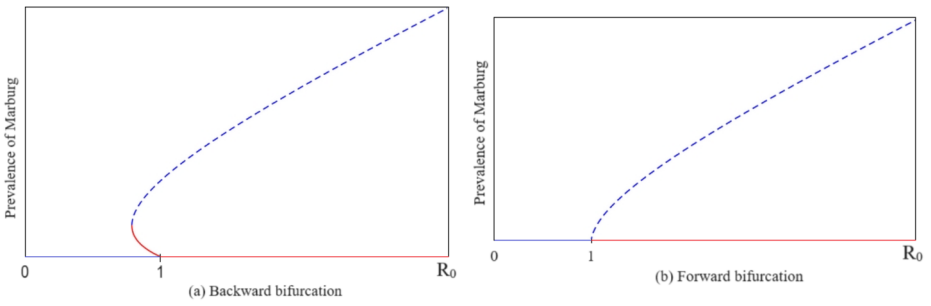

Figure 2 Backward and forward bifurcation diagram in the plane $R_0(\beta^{\dagger})$

partial derivatives of f as

$$\begin{aligned} a &= \nu_3 w_1 w_4 \frac{\partial^2 f_3}{\partial S \partial I} + \nu_3 w_2 w_4 \frac{\partial^2 f_3}{\partial V \partial I}, \\ &= \nu_3 w_4 [\beta w_1 + \beta w_2], \\ &= (1)\left(\frac{\sigma}{\alpha+\eta+\theta+\mu}\right)\left[\frac{\beta(\mu+\sigma)}{\mu+\xi} + \frac{\beta(\xi+\mu\rho)(\mu+\sigma)}{\mu^2(1-\rho)}\right], \\ &= \left(\frac{\sigma}{\alpha+\eta+\theta+\mu}\right)\left[\frac{\beta(\mu+\sigma)}{\mu+\xi} + \frac{\beta(\xi+\mu\rho)(\mu+\sigma)}{\mu^2(1-\rho)}\right] > 0, \end{aligned} \tag{23}$$

and

$$\begin{aligned} b &= \frac{\partial^2 f_3}{\partial I \partial \beta} = S + V, \\ &= \frac{\lambda(1-\rho)}{(\mu+\xi)} + \frac{\lambda(\xi+\mu\rho)}{\mu(\mu+\xi)} > 0, \quad \text{where} \quad 0 \le \rho \le 1. \end{aligned}$$

We observe from the result that $a > 0$ and $b > 0$. Per Theorem 4.1 in [10], for $a > 0$ and $b > 0$, the system exhibit a locally asymptotically stability as well as a positive unstable equilibrium and a negative, asymptotically stable equilibrium, as affirmed in Equation (18). Moreover, for $a > 0$, there exists a backward bifurcation occurring at $R_0 = 1$, which is an indication that reducing R_0 just below unity will not be adequate to control the spread of Marburg, as there will be multiplicity of endemic equilibrium. Finally, we observed that a forward bifurcation is achieved if the inequality (23) is reversed. We found that when the vaccination rate is too low (such that the proportion of immunized or vaccinated people in the MFE is not higher than the computed value $\beta^{\dagger}$), the backward bifurcation behavior of system (2) emerges. This scenario is shown in Fig. 2.

3.5 Sensitivity analysis

Sensitivity analysis is used to identify the factors that effectively reduce the transmission of infectious diseases. Forward sensitivity analysis is an essential aspect of disease modeling, but it may be challenging to compute for complicated biological models. Both ecologist and epidemiologist have shown significant interest in doing sensitivity analysis. The three common ways for calculating the sensitivity indices are [1.] using the linearizing system and solving the resulting set of linear algebraic equations, [2.] using a Latin hypercube sampling (LHS) approach, and [3.] using direct differentiation. Since the LHS technique uses the

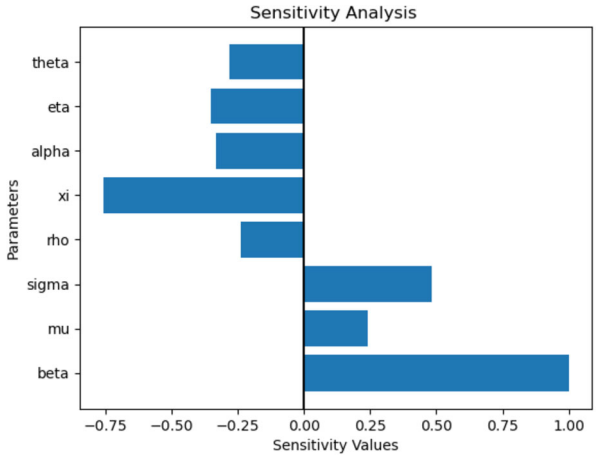

Figure 3 Sensitivity analysis of the basic reproduction number to changes in the parameters using PRCC index

partial Rank Correlation Coefficients (PRCCs) to calculate the sensitivity indices for each parameter value, we utilize it. The indices provide us with crucial information about the relative change of the parameters and R_0 in addition to illustrating the impact of several factors linked to the development of MVD, which subsequently aids in creating control strategies. Figure 3 displays the tornado plot for the normalized sensitivity index after a 1000 simulation run.

Figure 3 shows that the parameters β, μ and σ have a positive influence on the reproduction number, which describe that the growth or decay of these parameters say by 10% will increase or decrease the reproduction number by 10%, 2.5% and 5%, respectively. Hence, an increase in these parameters makes $R_0 > 1$ and forces system (2) to settle at the endemic state, leading to the persistence of MVD. On the other hand, the index for parameters θ, η, α, ξ and ρ illustrates that increasing these parameters will cause $R_0 < 1$ and enhance MVD eradication.

4 The control problem analysis

In this section, we modify system (2) by adding four control functions, denoted as $c_1(t)$, $c_2(t)$, $c_3(t)$ and $c_4(t)$ to generate system (24);

$$\begin{aligned}
\frac{dS}{dt} &= (1-\rho)\lambda - (1-c_1)\Psi S - (\mu + c_3\xi)S,\\
\frac{dV}{dt} &= \lambda\rho + c_3\xi S - (1-c_1)\Psi V - \mu V,\\
\frac{dE}{dt} &= (1-c_1)\Psi(S+V) - (\mu+\sigma)E,\\
\frac{dI}{dt} &= \sigma E - (c_4\alpha + c_2\theta + (1-c_2)\eta + \mu)I,\\
\frac{dT}{dt} &= c_4\alpha I - (\omega+\mu)T,\\
\frac{dR}{dt} &= c_2\theta I + \omega T - \mu R,
\end{aligned} \tag{24}$$

$$\frac{dD}{dt} = (1 - c_2)\eta I,$$

and the corresponding control reproduction number denoted as R_0^C derived as:

$$R_0^C = \frac{\beta\mu\sigma(1 - c_1)(1 - \rho)}{(\mu + c_3\xi)(\mu + \sigma)(c_4\alpha + (1 - c_2)\eta + c_2\theta + \mu)}. \tag{25}$$

The parameter $c_1(t)$ measures the level of success achieved through screening the population, while $c_2(t)$ assess the success of preventive measures such as avoiding; [1.] contact with blood and body fluids (such as urine, feces, saliva, sweat, vomit, etc.), [2.] items that may have come in contact with an infected person's blood or body fluids (such as clothes, bedding, needles, and medical equipment) and [3.] funeral or burial practices that involve touching the body of someone who has died from suspected or confirmed MVD. While some experimental vaccines have previously been tested, none have proven to be both highly effective and to provide durable one-time protection, however, we incorporate the parameter $c_3(t)$ to measure the success that will be achieved if stakeholders engage in the implementation of continuously vaccinating individuals. The parameter $c_4(t)$ represents continuously treating of infected individuals. In the scenario where $c_1 = c_2 = c_3 = c_4 = 1$, it may be inferred that the collection of time-dependent control variables exhibits complete efficacy in achieving the intended objective. However, if the values of c_1, c_2, c_3, and c_4 are all equal to zero, it can be inferred that the interventions being considered lack effectiveness. Furthermore, our objective is to identify the measures that might effectively reduce the overall number of affected individuals while keeping the associated expenses relatively low. Therefore, we establish an objective functional, denoted as $\mathcal{J}$, comprising positive values M_1, M_2, and M_3, which serves to equilibrate the coefficients of the infected state variables. When considering the objective functional, it is important to take into account a set of plausible interventions (c_1, c_2, c_3, c_4) within the time range $[0, T_F]$. Therefore,

$$\begin{aligned}&\mathcal{J}(c_1, c_2, c_3, c_4)\\ &\quad = \int_0^{T_F} \left[M_1E(t) + M_2I(t) + M_3D(t) + \frac{W_1c_1^2(t)}{2} + \frac{W_2c_2^2(t)}{2} + \frac{W_3c_3^2(t)}{2} + \frac{W_4c_4^2(t)}{2}\right]dt,\end{aligned} \tag{26}$$

where W_1, W_2, W_3 and W_4 are weight constants on the controls. The necessary criteria for the optimal controls can be derived by applying Pontryagin's Maximum Principle as demonstrated in [16]. The issue at hand is the minimization of the Hamiltonian ($\mathcal{H}$) in relation to the provided controls. Hence,

$$\begin{aligned}\mathcal{H} = &\left[M_1E(t) + M_2I(t) + M_3D(t) + \frac{W_1c_1^2(t)}{2} + \frac{W_2c_2^2(t)}{2} + \frac{W_4c_4^2(t)}{2}\right] +\\ &\Gamma_S[(1 - \rho)\lambda - (1 - c_1)\Psi S - (\mu + c_3\xi)S] +\\ &\Gamma_V[\lambda\rho + c_3\xi S - (1 - c_1)\Psi V - \mu V] +\\ &\Gamma_E[(1 - c_1)\Psi(S + V) - (\mu + \sigma)E] +\\ &\Gamma_I[\sigma E - c_2\theta I - ((1 - c_2)\eta + \mu)I - c_4\alpha I] +\\ &\Gamma_T[c_4\alpha I - (\omega + \mu)T] +\end{aligned}$$

$$\Gamma_R[c_2\theta I + \omega T - \mu R] +$$
$$\Gamma_D[(1-c_2)\eta I].$$

The parameters $\Gamma_S, \Gamma_V, \Gamma_E, \Gamma_I, \Gamma_T, \Gamma_R, \Gamma_D$ are the costate variables associated with the respective state variables $S(t), V(t), E(t), I(t), T(t), R(t), D(t)$. There exist an adjoint function such that:

$$\begin{aligned}
\frac{d\Gamma_S}{dt} &= (1-c_1)\beta I(\Gamma_S - \Gamma_E) + (1-c_1)\delta\beta D(\Gamma_S - \Gamma_E) + c_3\xi(\Gamma_S - \Gamma_V) + \Gamma_S\mu,\\
\frac{d\Gamma_V}{dt} &= (1-c_1)\beta I(\Gamma_V - \Gamma_E) + (1-c_1)\delta\beta D(\Gamma_V - \Gamma_E) + \Gamma_V\mu,\\
\frac{d\Gamma_E}{dt} &= -M_1 + (\Gamma_E - \Gamma_I)\sigma + \Gamma_E\mu,\\
\frac{d\Gamma_I}{dt} &= -M_2 + c_2\theta(\Gamma_I - \Gamma_R) + c_4\alpha(\gamma_I - \Gamma_T) + (1-c_2)\eta(\Gamma_I - \Gamma_D) + \Gamma_I\mu,\\
\frac{d\Gamma_T}{dt} &= \omega(\Gamma_T - \Gamma_R) + \Gamma_T\mu,\\
\frac{d\Gamma_R}{dt} &= \Gamma_R\mu,\\
\frac{d\Gamma_D}{dt} &= -M_3.
\end{aligned} \tag{27}$$

The following relations are used to derive Equation (27);

$$\begin{aligned}
&\frac{d\Gamma_S}{dt} = -\frac{\partial\mathcal{H}}{dS}, \quad \frac{d\Gamma_V}{dt} = -\frac{\partial\mathcal{H}}{dV}, \quad \frac{d\Gamma_E}{dt} = -\frac{\partial\mathcal{H}}{dE}, \quad \frac{d\Gamma_I}{dt} = -\frac{\partial\mathcal{H}}{dI}, \quad \frac{d\Gamma_T}{dt} = -\frac{\partial\mathcal{H}}{dT},\\
&\frac{d\Gamma_R}{dt} = -\frac{\partial\mathcal{H}}{dR}, \quad \frac{d\Gamma_D}{dt} = -\frac{\partial\mathcal{H}}{dD}.
\end{aligned}$$

The relevant transversality conditions $\Gamma_S(t) = 0$, $\Gamma_V(t) = 0$, $\Gamma_E(t) = 0$, $\Gamma_I(t) = 0$, $\Gamma_T(t) = 0$, $\Gamma_R(t) = 0$, and $\Gamma_D(t) = 0$ holds such that, for $\frac{\partial H}{\partial c_i}$, where $i = 1, 2, 3, 4$, gives

$$\begin{aligned}
\frac{\partial\mathcal{H}}{\partial c_1} &= W_1c_1 + \beta IS(\Gamma_S - \Gamma_E) + \beta\beta DS(\Gamma_S - \Gamma_E) + \beta IV(\Gamma_V - \Gamma_E) + \delta\beta DV(\Gamma_V - \Gamma_E) = 0,\\
\frac{\partial\mathcal{H}}{\partial c_2} &= W_2c_2 + \theta I(\Gamma_I - \Gamma_R) + \eta I(\Gamma_I - \Gamma_D) = 0,\\
\frac{\partial\mathcal{H}}{dt} &= W_3c_3 + \xi S(\Gamma_S - \Gamma_V) = 0,\\
\frac{\partial\mathcal{H}}{\partial c_4} &= W_4c_4 + \alpha I(\gamma_I - \Gamma_T) = 0.
\end{aligned} \tag{28}$$

From Equation (28), we obtain

$$\begin{aligned}
c_1 &= \frac{\beta IS(\Gamma_E - \Gamma_S) + \delta\beta DS(\Gamma_E - \Gamma_S) + \beta IV(\Gamma_E - \Gamma_V) + \delta\beta DV(\Gamma_E - \Gamma_V)}{W_1},\\
c_2 &= \frac{\theta I(\Gamma_R - \Gamma_I) + \eta I(\Gamma_D - \Gamma_I)}{W_2},\\
c_3 &= \frac{\xi S(\Gamma_V - \Gamma_S)}{W_3},
\end{aligned} \tag{29}$$

$$c_4 = \frac{\alpha I(\Gamma_T - \Gamma_I)}{W_4}.$$

From Equation (29), whenever $0 < c_i < 1$, we have

$$\begin{aligned}
c_1^*(t) &= \min\left\{\max\left\{0, \frac{\beta IS(\Gamma_E - \Gamma_S) + \delta\beta DS(\Gamma_E - \Gamma_S) + \beta IV(\Gamma_E - \Gamma_V) + \delta\beta DV(\Gamma_E - \Gamma_V)}{W_1}\right\}, 1\right\},\\
c_2^*(t) &= \min\left\{\max\left\{0, \frac{\theta I(\Gamma_R - \Gamma_I) + \eta I(\Gamma_D - \Gamma_I)}{W_2}\right\}, 1\right\},\\
c_3^*(t) &= \min\left\{\max\left\{0, \frac{\xi S(\Gamma_V - \Gamma_S)}{W_3}\right\}, 1\right\},\\
c_4^*(t) &= \min\left\{\max\left\{0, \frac{\alpha I(\Gamma_T - \Gamma_I)}{W_4}\right\}, 1\right\}.
\end{aligned} \tag{30}$$

4.1 Parameter estimation

To get the numerical findings from our analysis of the prevalence and trends of MVD, we estimated the parameter values in system (22) in this subsection. The data used were from Equatorial Guinea. There have been reports of 17 laboratory-confirmed cases of MVD and 23 suspected cases in Equatorial Guinea between December 19 and May 1, 2023, as shown in Fig. 4. Reports of the latest verified case date back to April 20. From this data, we analyzed the confirmed cases of MVD infection reported in the country.

The Nelder–Mead optimization technique was used to estimate the parameters. Minimizing the mean squared error (MSE) between the predicted states and their observation values from the data was the aim of the least-squares regression technique. Equation (31) illustrates how to minimize the total squared error that exists between the data and model.

$$\min M(\mathcal{P}) = \sum_{i=1}^{n} [\bar{y}(t_i, \mathcal{P}) - y(t_i)]^2, \tag{31}$$

where y and $\mathcal{P}$ denotes the state variable and model parameters, respectively. The goal is to minimize the sum of difference between the observed data points $y(t_i)$, (in this model I)

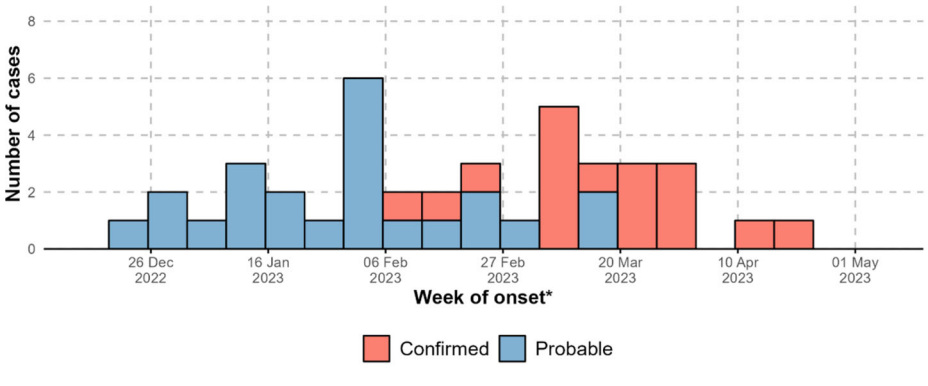

Figure 4 Weekly distribution of MVD cases based on the onset of symptoms* and case categorization in Equatorial Guinea, from 19th December to 1st May 2023

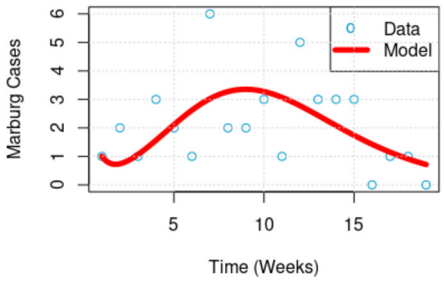

Figure 5 Fitted model of system (2) using the Nelder–Mead optimization approach

Table 1 Model parameters and their estimated values

Parameters	Values (per/day)	Reference	Parameters	Values (per/day)	Reference
λ	0.455	[4]	ξ	0.285	Assumed
ρ	0.192	[7]	σ	0.094	Estimated
β	0.032	Estimated	α	0.913	Estimated
δ	$1e^{-7}$	Assumed	θ	0.776	Estimated
μ	0.088	[7]	η	0.967	Estimated
ω	0.014	Assumed			

and the solution of $\bar{y}(t_i, \mathcal{P})$, (that is, System (2)), associated with the model parameter $\mathcal{P}$. Executing Equation (31) in *R-software* with the help of deSolve and the FME package, we are able to estimate the parameter values. Figure 5 shows the estimated model fit, while Table 1 shows the parameter values.

4.2 Results

This part presents the simulation results of the Marburg model presented in this study. The analysis includes evaluation of the effectiveness of different preventive strategies, comparing the model with (Equation (24)) and without control (Equation (2)). Table 1, depicts parameter values used in simulating and $M_1 = 50$; $M_2 = 50$; $M_3 = 2$; and $W_1 = 5$; $W_2 = 10$; $W_3 = 15$; $W_4 = 20$ describes the weights and balancing constants respectively. The associated values for the state variables are $S = 400$, $V = 90$, $E = 40$, $I = 0$, $T = 50$, $R = 20$ and $D = 0$.

Simulation of the model is done by examining four distinct scenarios in order to assess the efficacy and consequences of each control approach on the incidence of the disease. The scenarios presented in this study are designed using several intervention approaches, specifically those using single, coupled, tripled, and fourfold control variables. In the subsequent analysis, we delve into a comprehensive examination of the visual effects associated with each individual situation.

4.3 1st intervention: application of a single control

The initial approach is selected in a manner that exclusively employs just one control at each given moment.

4.3.1 Implementation of screening only

This intervention is achieved by setting $c_1 \neq 0$, which deals with the isolation of suspected infected individuals to optimize the objective function while the controls $c_2 = c_3 = c_4 = 0$. Figures 6a and 6b depict this situation. Screening helps protect the public by preventing exposure to people who may have the MVD. Figure 6b shows that effective screening of

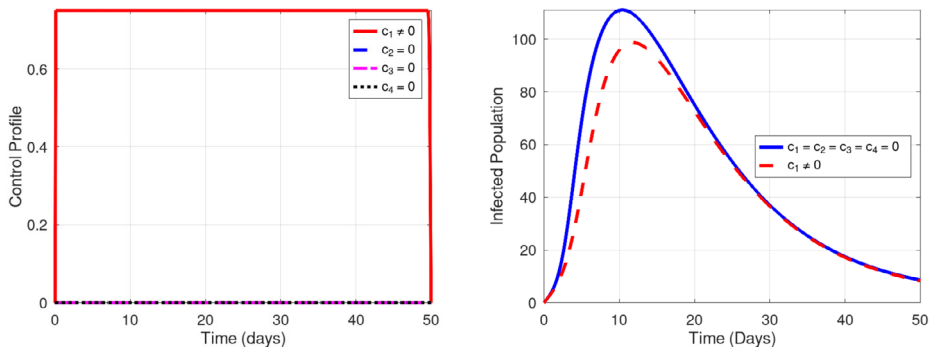

(a) Control profile (b) Infected population.

Figure 6 Effect of using isolation as the sole strategy. It is observed from (a) that it is imperative to conduct regular screenings for the entire population believed to be potentially infected with the virus in order to effectively eliminate the disease. The effect and efficacy of this method of control can be observed through the reduction in the number of (b) infected individuals

individuals who may have or come into contact with an MVD person will help reduce the rate of MVD infection. It can further be seen from Fig. 6b that, in the natural settings it is difficult to straightaway identify individuals with MVD or those that had contact with an MVD person, hence, there is an initial increase in the infected population, but after 10 days where clear symptoms begin to show and this control measure takes place, it leads to a reduction in the infected population. Figure 6a also shows that to sustain and reduce infection, this control measure, c_1, should be maintained intensively throughout the period of disease persistence.

4.3.2 Implementation of prevention only

In this methodology, the optimization of the objective function is achieved by exclusively implementing the control c_2, which pertains to prevention. The controls c_2, c_3, and c_4 are all assigned a value of zero, as depicted in Fig. 7. In order to enhance infection control measures, it is recommended, as depicted in Fig. 7a, that c_2 be consistently maintained at a high level over the initial thirty-two day period. That is, individuals should implement this strategy slightly beyond the 21 day incubation period. This will help prevent transmission of the disease, as shown in Fig. 7b.

4.3.3 Implementation of continuous vaccination only

A safe and effective vaccine is an important tool to protect and prevent the introduction and spread of MVD in the population. We set $c_3 \neq 0$ and $c_1 = c_2 = c_4 = 0$ to optimize the objective function. As can be observed from Fig. 8, implementing this control measure at the optimum level help to mitigate the spread of MVD, as shown by the significant decrease in the infected compartment (*see Fig. 8b*). Moreover, Fig. 8a indicates that, the whole population is required to be continually vaccinated throughout the entire period of disease persistence to achieve the result in Fig. 8b, which shows that immediately after the incubation period the entire population settles at the Marburg-free equilibrium state.

4.3.4 Implementation of continuous treatment only

Although there is no specific treatment for MVD, historical fatality rates have been high and, based on recent experience with Ebola, various studies such as [17] asserted that

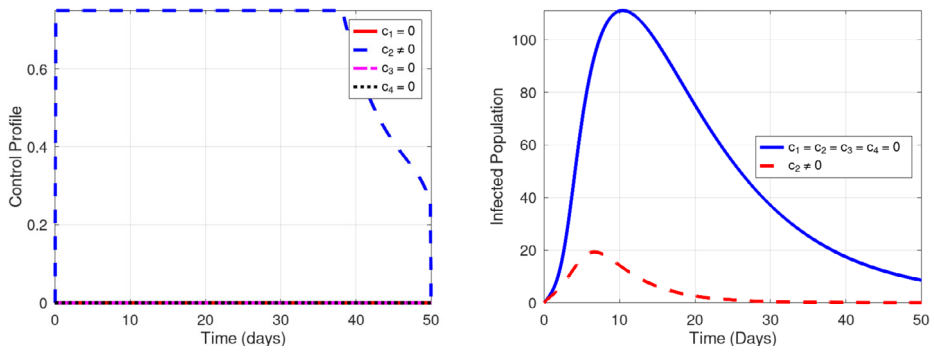

(a) Control profile (b) Infected population.

Figure 7 The impact of employing prevention as the exclusive approach. It can be noted from the data that c_2 should be consistently maintained over a duration of 32 days. The control technique has demonstrated its impact and effectiveness by the observed reduction in the number of individuals who are infected

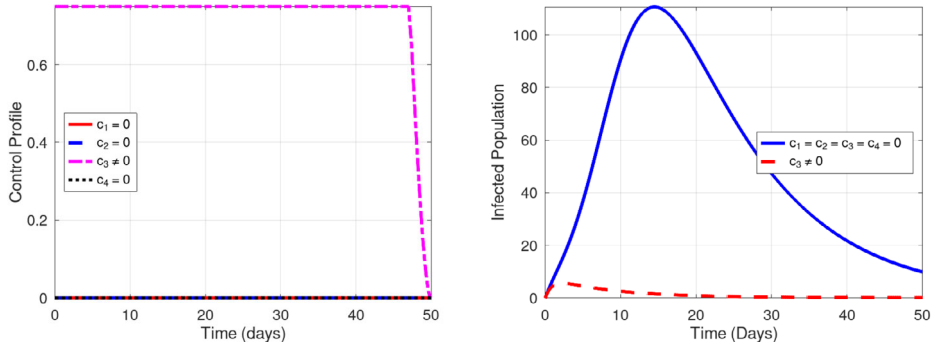

(a) Control profile (b) Infected population.

Figure 8 Effect of using continuous vaccination as the sole strategy. It is observed from (a) that c_3 should be sustained intensively for the entire period of disease persistence. The reduction in the number of infected persons in (b) demonstrates the significance and efficiency of this management technique

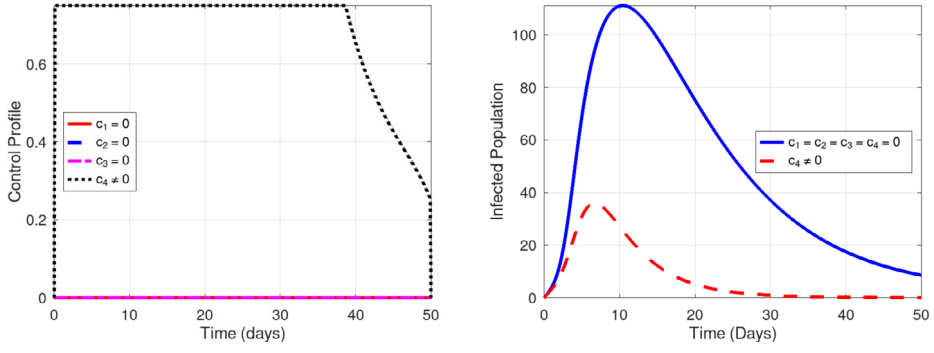

(a) Control profile (b) Infected population.

Figure 9 Effect of using continuous treatment as the sole strategy. It is observed from (a) that individuals should be continually treated for the first 35 days before reducing it to about 25% of the individuals. The decrease in (b) demonstrates the influence and efficacy of this method of management

MVD may be improved with aggressive supportive care and fluid resuscitation. According to the WHO and CDC, this measure has been successfully employed on MVD. Therefore, Fig. 9 provides evidence for the effectiveness of this control technique, as demonstrated by the notable drop observed in Fig. 9b. Furthermore, Fig. 9a depicts that to sustain this strategy, 100% of infected individuals are to be treated right from the onset to about 35 days, which then can be reduced to about 25%.

4.4 2nd intervention: application of two controls

Using coupled controls, we look into what happens when we use both of these controls simultaneously. Six different strategies are implemented under this subsection. They are described in details as follows:

4.4.1 Implementation of screening and prevention only

The strategy applied in this section requires $c_1 = c_2 \neq 0$, while $c_3 = c_4 = 0$. Figure 10a shows the optimal solutions for this strategy. It can be observed from Fig. 10a that if both screening and prevention is implemented for 45 days, the level of infection in the population reduces as shown in Fig. 10b. It can further be deduced that the population settles at the disease-free state after 20 days when these strategies are applied.

4.4.2 Implementation of screening and continuous vaccination only

Based on the findings in [18], it has been established that vaccination has the ability to enhance the immune system of individuals. Hence, the implementation of ongoing vaccination and screening measures can effectively mitigate the prevalence of illness and limit its transmission among persons. Figure 11a depicts that screening should begin from the very moment MVD is announced and maintained throughout the entire period of disease persistence, while 100% of the population are to be vaccinated for about 46 days throughout the 50 days target period. People who receive vaccination are much less likely to experience severe symptoms than people who are not, however, it is possible for people to be infected after being vaccinated and can spread MVD. Hence, as indicated by Fig. 11b, the system does not achieve a disease-free state.

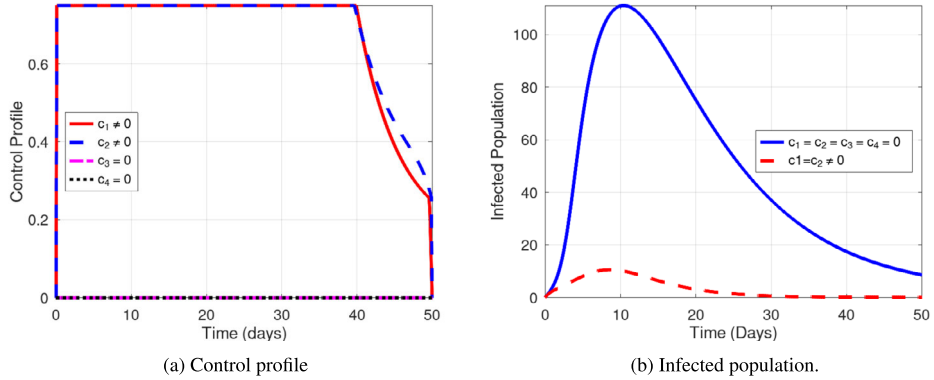

(a) Control profile (b) Infected population.

Figure 10 Effect of using both screening and prevention as the sole strategy. (a) Control profile indicating that both screening and prevention should be sustained for 45 days right from the onset of the disease. The control technique has demonstrated its impact and effectiveness by the observed reduction in the number of individuals who are infected

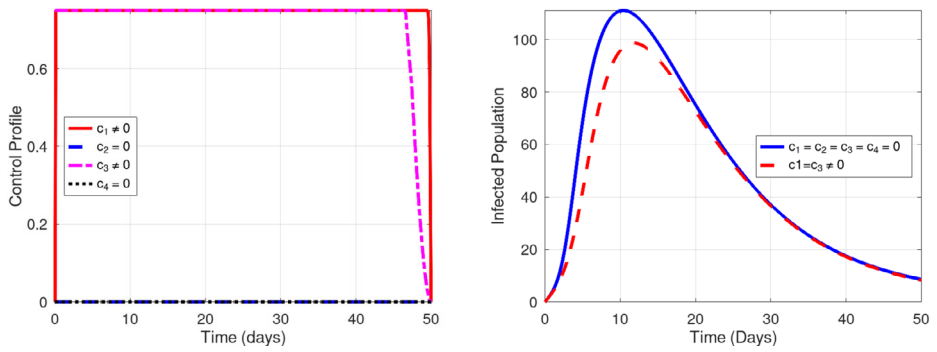

(a) Control profile (b) Infected population.

Figure 11 Effect of using both screening and continuous vaccination as the sole strategy. It is observed from (a) that screening should be sustained intensively throughout the entire period of disease persistence, and (b) described the influence of this control strategy in decreasing the infected number of individuals

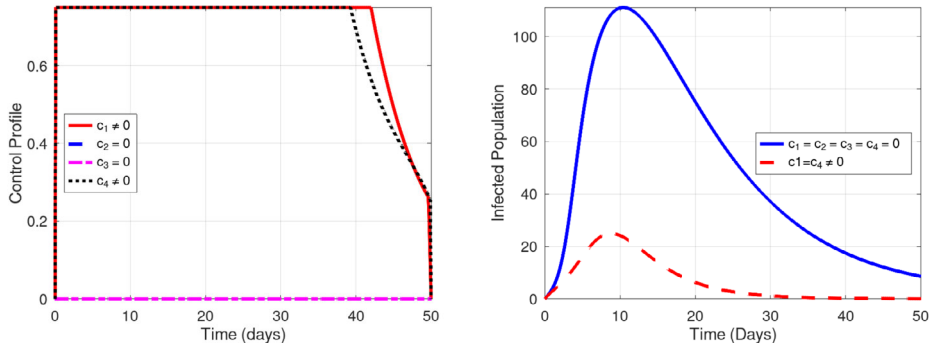

(a) Control profile (b) Infected population.

Figure 12 Effect of using both screening and continuous vaccination as the sole strategy. It is observed from (a) that screening should be sustained intensively throughout the entire period of disease persistence and (b) described the effect of this control strategy in decreasing the infected number of individuals

4.4.3 Implementation of screening and continuous treatment only

When both screening and continuous treatment only are applied, the optimal solution obtained are shown in Fig. 12. In a screen-and-treat approach, treatment is provided based on a positive outcome of a primary screening test. Figure 12a shows that screening should be implemented from onset of disease to about 42 days, slightly above the incubation period of MVD, while treatment should be implemented for about 40 days. As shown in Fig. 12b, this explains the fact that within the incubation period of the MVD, infected individuals will be detected and provided with the needed treatment as a result the system settles to the MFE state immediately after the duration of the incubation period of MVD.

4.4.4 Implementation of prevention and continuous vaccination only

The outcomes generated by system (24) with control demonstrate a noteworthy reduction in infection incidence when compared to the outcomes of system (2) without control, as illustrated in Fig. 13b. Figure 13a provide the time duration required for implementing these strategies, such that prevention is required to be strictly employed for 37 days and

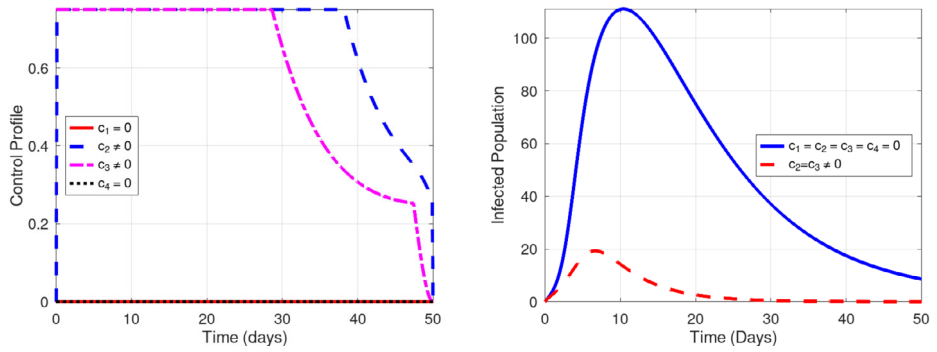

(a) Control profile (b) Infected population.

Figure 13 Effect of using both prevention and continuous vaccination as the sole strategy. It is observed from (a) that prevention should be sustained intensively for 37 days and 29 days for vaccination. (b) Describes the influence of this control strategy in decreasing the infected number of individuals

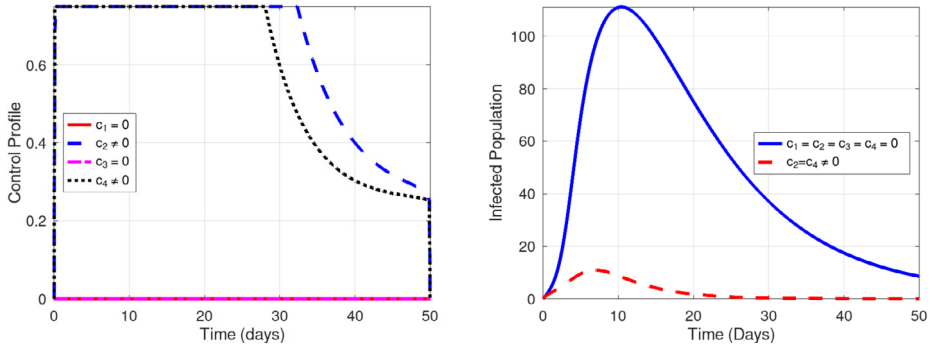

(a) Control profile (b) Infected population.

Figure 14 Effect of using both prevention and continuous treatment as the sole strategy. It is observed from (a) that prevention should be sustained intensively for 32 days and 28 days for treatment. (b) described the influence of this control strategy in decreasing the infected number of individuals

continuous vaccination is to be sustained for 29 days. When this is done, it is observed from Fig. 13b that the system will achieve a Marburg-free equilibrium state after 20 days.

4.4.5 Implementation of prevention and continuous treatment only

Prevention techniques help stops an infection or sickness before it starts, while treatment normally begins either before signs and symptoms of the disease occur, or shortly thereafter. Applying prevention and continuous treatment as the control strategy in this section show that it is effective in reducing the infected population, as shown in Fig. 14b.

4.4.6 Implementation of continuous vaccination and continuous treatment

Figure 15 shows the optimal solution when continuous vaccination and treatment are applied. The result from Fig. 15a shows that the entire population are to be vaccinated and sustained for 35 days, while infected individuals are to receive treatment and sustained for 38 days to achieve a MFE state, as shown in Fig. 15b.

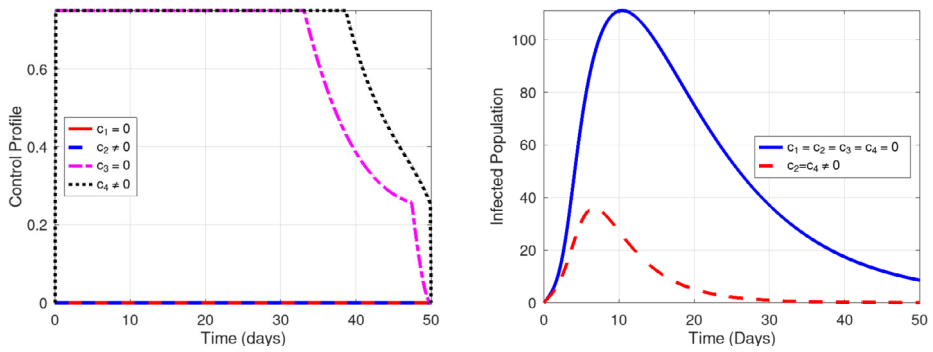

(a) Control profile (b) Infected population.

Figure 15 The outcome of employing a combined strategy of continual immunization and therapy. From (a), we learn that the entire population must undergo vaccination and treatment for 35 and 38 days, respectively. (b) outlined how this technique helps to reduce the number of infected people in the population

4.4.7 3rd intervention: application of three controls

The third case illustrates the effect that tripartite controls have on the dynamical relationships between model state variables. An optimal solution when screening, prevention and continuous vaccination are employed is shown in Figs. 16a and 16b. In addition, Figs. 16c and 16d show the solution when screening, continuous vaccination and continuous treatment are implemented, while the optimal solution for the combined implementation of prevention, continuous vaccination and treatment are shown in Figs. 16e and 16f. Each of the combined threefold strategy was seen to be effective as in all situation there was a decrease in the infected number of individuals.

4.4.8 4th intervention: implementation of all controls

Finally, with this approach, all the controls c_1, c_2, c_3 and c_4 are activated to optimize the objective function, observed in Fig. 17b. Figure 17b illustrates that the activation of all controls leads to a reduction in effort and time required to mitigate MVD infection. The system reaches the MFE more rapidly compared to other measures. However, it is necessary to implement a 17-day intensive vaccination regimen for those who have been exposed to MVD. Furthermore, in the case that all controls are to be enacted, it is necessary to administer intensive treatment for a duration of 21 days. Additionally, preventive measures and screening protocols should be performed for 23 and 30 days, respectively, ensuring that the incubation period for MVD has ended by that time. Thus, it is anticipated that in order to develop an economically efficient approach for a successful intervention, equal consideration should be given to all four controls simultaneously.

Relying on Equation (25) and values from Table 1, we observed from Table 2 that when the various intervention measures are applied, the long term behaviour of the controlled system implies a drastic and complete eradication of MVD from the system, which prevents a possible reoccurrence of the disease after it finite time (T_F).

4.5 Cost-effectiveness analysis

Finding the most cost-effective optimal control measure among the single and combined strategies of the four established control measures is crucial for minimizing the spread of MVD at the lowest possible cost. In order to investigate cost-effectiveness analyses, the

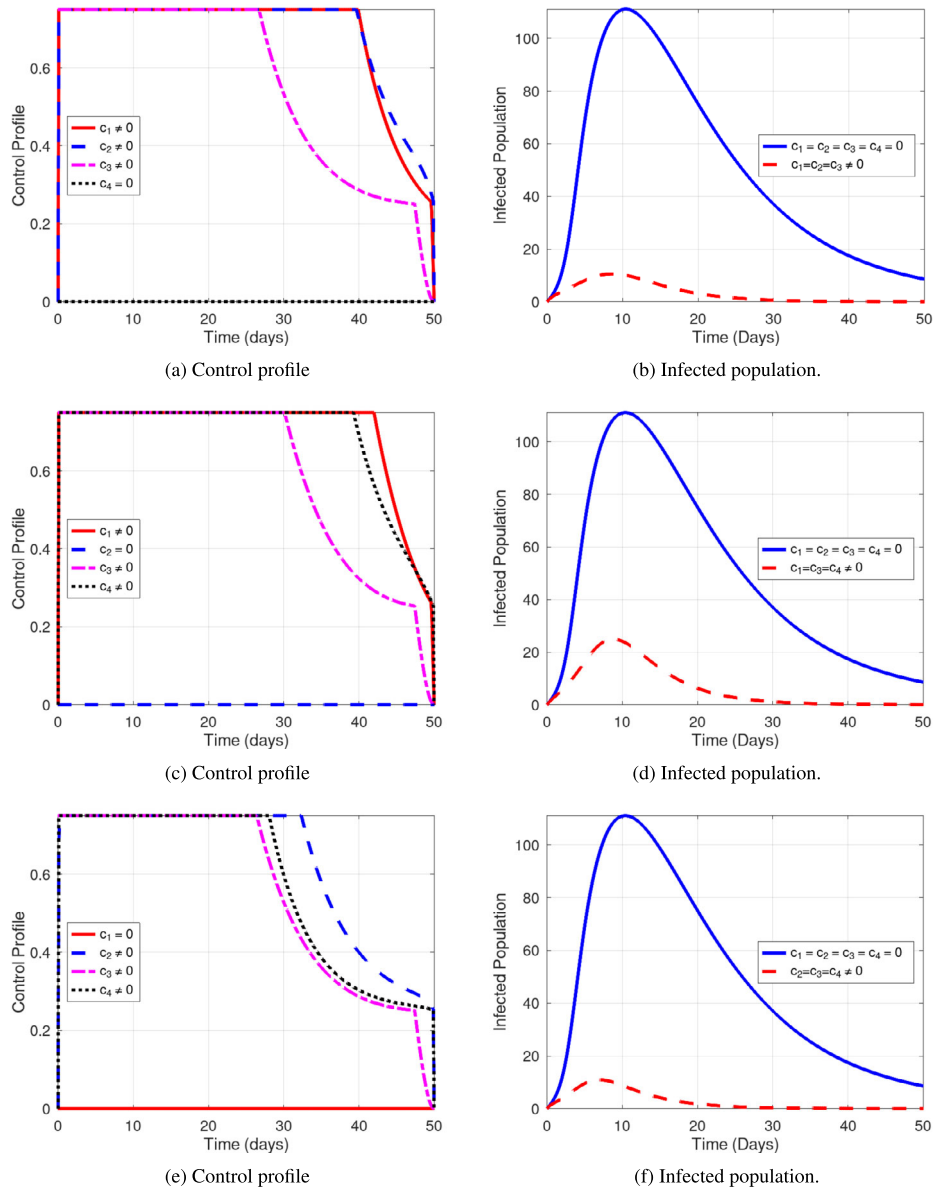

(a) Control profile (b) Infected population.

(c) Control profile (d) Infected population.

(e) Control profile (f) Infected population.

Figure 16 Effect of using three combined strategy at a go. (a) Control profile for implementing screening, prevention and continuous vaccination with its associated influence shown in (b). The control profile for the combined effect of screening, continuous vaccination and continuous treatment is given in (c), and (d) depicts the corresponding effectiveness of this intervention. (e) is the control profile for collectively implementing prevention, continuous vaccination and continuous treatment with the associated effect given in (f)

incremental cost effectiveness ratio (ICER) is used. To make sure that limited resources are used wisely, ICER is used to compare two competing strategies for halting the spread of disease or other related problems. As stated, the ICER formula is established as

$$\text{ICER} = \frac{\text{Differences in total costs between control measures}}{\text{Differences in total number of Marburg infection averted by control measures}}. \tag{32}$$

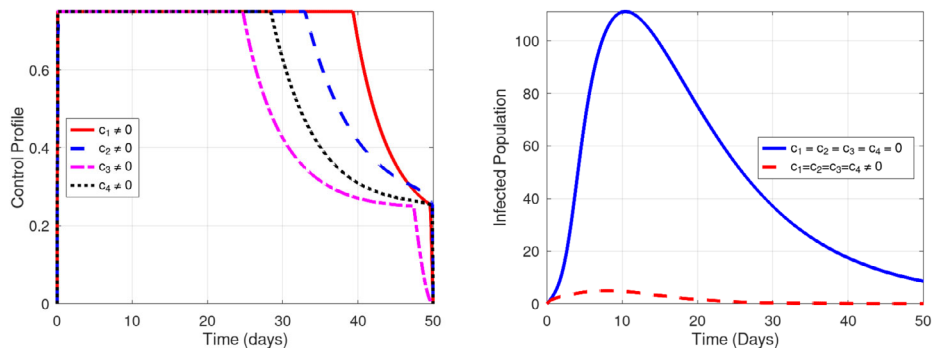

(a) Control profile (b) Infected population.

Figure 17 Effect of using all controls

Table 2 Results of the control reproduction number after each intervention

Intervention	Control measure(s)	R_0^C
1st interventions	S only ($c_1 \neq 0$)	0
	P only ($c_2 \neq 0$)	0.0008099
	V only ($c_3 \neq 0$)	$9.183687e^{-06}$
	T only ($c_4 \neq 0$)	0.00044279
2nd interventions	S and P only ($c_1 = c_2 \neq 0$)	0
	S and V only ($c_1 = c_3 \neq 0$)	0
	S and T only ($c_1 = c_4 \neq 0$)	0
	P and V only ($c_2 = c_3 \neq 0$)	0.000191083
	P and T only ($c_2 = c_4 \neq 0$)	0.00121379
	V and T only ($c_3 = c_4 \neq 0$)	0.000104464
3rd interventions	S, P and V only ($c_1 = c_2 = c_3 \neq 0$)	0
	S, V and T only ($c_1 = c_3 = c_4 \neq 0$)	0
	P, V and T only ($c_2 = c_3 = c_4 \neq 0$)	0.000286364
4th intervention	S, P, V, T ($c_1 = c_2 = c_3 = c_4 \neq 0$)	0

The cost of implementing control measures can be determined by using objective functional in Equation (26), while the number of infections averted can be calculated by comparing the number of infectious individuals with and without control measures. Table 3 present the ICER result in ascending order of the total infection averted for each control measure implemented. However, as asserted by [REF] that a single intervention cannot be relied upon to entirely eliminate the transmission of a disease from the population, we aligned with this assertion and did not evaluate methods that apply just one intervention. Hence, following is an order for pairwise comparisons of the multi-intervention techniques as described in Table 3. Let S, P, V and T denote the associated control measure for screening, prevention, continuous vaccination and continuous treatment, respectively.

Following Table 3, the ICER values were obtained as follows:

$$\text{ICER}_{(\text{P and V})} = \frac{7.9948 \times 10^5}{7.3281 \times 10^4} = 1.09 \times 10^1,$$

$$\text{ICER}_{(\text{S, P and V})} = \frac{7.9754 \times 10^5 - 7.9948 \times 10^5}{7.5225 \times 10^4 - 7.3281 \times 10^4} = -9.979 \times 10^{-1},$$

$$\text{ICER}_{(\text{P, V and T})} = \frac{7.9553 \times 10^5 - 7.9754 \times 10^5}{7.7234 \times 10^4 - 7.5225 \times 10^4} = -1.000,$$

Table 3 ICER values incorporating the infections averted and its associated cost for each control measure

Control measures	Total infection averted	Total costs	ICER
P and V only	7.3281*e* + 04	7.9948*e* + 05	1.09×10^1
S, P and V only	7.5225*e* + 04	7.9754*e* + 05	–0.998
S and P only	7.5225*e* + 04	7.9754*e* + 05	–
P, V and T only	7.7234*e* + 04	7.9553*e* + 05	–1.000
S, P, V and T	7.9158*e* + 04	7.9360*e* + 05	–1.003
S, P, and T	7.9158*e* + 04	7.9360*e* + 05	–
S and V only	7.9877*e* + 04	7.9288*e* + 05	–1.001
V and T only	8.1894*e* + 04	7.9087*e* + 05	–.0997
S and T only	8.3829*e* + 04	7.8893*e* + 05	–1.003
S, V and T only	8.3829*e* + 04	7.8893*e* + 05	–

$$\mathrm{ICER}_{(\mathrm{S,\ P,\ V\ and\ T})} = \frac{7.0360 \times 10^5 - 7.9553 \times 10^5}{7.9158 \times 10^4 - 7.7234 \times 10^4} = -1.003,$$

$$\mathrm{ICER}_{(\mathrm{S\ and\ V})} = \frac{7.9288 \times 10^5 - 7.9360 \times 10^5}{7.9877 \times 10^4 - 7.9158 \times 10^4} = -1.001,$$

$$\mathrm{ICER}_{(\mathrm{V\ and\ T})} = \frac{7.9087 \times 10^5 - 7.9288 \times 10^5}{8.1894 \times 10^4 - 7.9877 \times 10^4} = -0.9965,$$

$$\mathrm{ICER}_{(\mathrm{S\ and\ T})} = \frac{7.8893 \times 10^5 - 7.9087 \times 10^5}{8.3829 \times 10^4 - 8.1894 \times 10^4} = -1.0026 \approx -1.003.$$

The control measures in Table 3 are ranked based on their effectiveness in controlling Marburg infections, from least to most effective. As a result implementing only prevention and vaccination averts the least, in terms of the, number of infections, while implementing screening, continuous vaccination and continuous treatment averted the highest number of infections in the population. It is important to state that in computing the ICER, due to the same number of infection averted for S, P, V and S, P; S, P, V, T and S, P, T; as well as S, T and S, V, T, the ICER is not compared between these control measures. However, Table 3 shows that the control measure incorporating prevention and continuous vaccination (P and V only) dominates the rest of the control measures, implying that P and V only is costly, hence, we eliminate $ICER_{(\mathrm{P\ and\ V})}$ and recalculate the ICER values for the closest value, which is V and T only, and S, P, V.

$$\mathrm{ICER}_{(\mathrm{V\ and\ T\ only})} = \frac{7.9087 \times 10^5}{8.1894 \times 10^4} = 9.657,$$

$$\mathrm{ICER}_{(\mathrm{S,\ P\ and\ V\ only})} = \frac{7.9754 \times 10^5 - 7.9087 \times 10^5}{7.5225 \times 10^4 - 8.1894 \times 10^4} = -1.000.$$

Table 4 shows that after recalculation, the ICER value for the V, T dominated that of S, P, V implying that implementing V, T only is more costly when compared to the implementation of S, P and V. Therefore, we exclude variables V and T from the pool of measures contending for scarce resources. Importantly, Table 4 shows that the ICER value for S, P, V when compared to remaining measures in Table 3 provide greater effectiveness at a cheaper cost except for P, V and T only which equally has an ICER value of –1.000. Hence, there is no requirement to recalculate the incremental cost-effectiveness ratio (ICER) for these alternative measures. However, it is observed that the two interventions avert different total number of infections such that the total infection averted by $SPV = 7.5225 \times 10^4$ while $PVT = 7.7234 \times 10^4$. Thus, should a decision be taken among these two measures,

Table 4 Comparing V, T only and S, P, V only

Control measures	Total infection averted	Total costs	ICER
V and T only	$8.1894e+04$	$7.9087e+05$	9.657
S, P and V only	$7.5225e+04$	$7.9754e+05$	−1.000

the best decision is to go for the combined measure of prevention, continuous vaccination and treatment, which has the potential to reduce the Marburg virus drastically and also offer greater effectiveness at a lower cost.

5 Discussion

Both Marburg and Ebola virus disease belong to the Filoviridae family, specifically classified as filoviruses. Despite being caused by distinct viruses, both diseases have comparable clinical characteristics. Both Marburg and Ebola viruses are infrequent occurrences and possess the potential to instigate epidemics characterized by elevated mortality rates. However, much work and studies have only been conducted on Ebola, providing comprehensive and thorough analysis on the disease propagation (*see [19]*). Due to their similarity, based on understanding obtained from the works done on Ebola, we investigated a mathematical model that provides a good description for the transmission of MVD incorporating vaccination and treatment. Our model results were in line with studies such as [6], which obtained a low basic reproduction from 0.5[95% *CI* 0.05 – 1.8] to 1.2[95% *CI* 1.0 – 1.9] when vaccination is applied. However, they also observed this result is accompanied with a high case fatality ratio; a situation our result contradicted. Based on Fig. 8a and Table 2, we observed that when vaccination only is applied as a control strategy, the control basic reproduction number obtained is $9.183687e^{-06}$ and this is associated with a decrease in the case fatality ratio after the incubation period (*see Fig. 8a*). The initial model without control parameters affirmed the importance of vaccination to be included in any stakeholder policy decision making. Because, both the qualitative analysis and region within which the model is reasonable showed that the occurrence of a bifurcation was shown to be as a result of reinfection and loss of immunity of vaccinated individuals. Further, we found that when the vaccination rate is too low (such that the proportion of immunized or vaccinated people in the MFE is not higher than the computed value $\beta^{\dagger}$), the backward bifurcation behavior of system (2) emerges. As a result, $R_0 < 1$ may not be sufficient to eradicate the transmission of MVD from the population. This was shown in the work of [6]. Furthermore, both our study and the work of [8], agreed to the fact that, treatment therapy is required in order to lower the amount of deaths brought on by MVD. It was observed that among the control strategies, continuous treatment helps play a major role in reducing the number of deaths due to MVD, but it is the least strategy when considering reducing the transmission of the disease, as it has the highest R_0 value (*see Table 2*). However, in general, just as affirmed by the work of [7], an increase in dissemination of information surrounding the activities of prevention plays a key role as a control strategy in reducing MVD transmission. The current study's findings agrees with the results of [7] and believed that in order to prevent and restrict the spread of Marburg virus, public policy makers need to focus on increasing the importance of information sharing on prevention. A unique composition in our study compared to other MVD studies was the fact that we performed a sensitivity analysis, which helped to identify the most sensitive and positively correlated parameters with the rate of disease transmission. These

parameters became the targets for adopting measures needed in controlling the spread of MVD. Thus, unlike the work of [8] and [7], which believed that a single or only two control measures are enough to eradicate MVD, it was deduced from the numerical results of the current study that the application of all four controls (screening, prevention, continuous vaccination and treatment) require less effort and time to reduce and eradicate MVD in the population. Because, there is the believe and assertion that it is possible to get a better understanding and even forecast the dynamics of infectious diseases by challenging, updating, and changing the constraints of long-standing concepts, theories, and practices in light of new scientific discoveries and unexpected physical occurrences, we employed ICER to determine the most cost-effective optimal control measure for the various controls. It was established that, the intervention that offered the greatest effectiveness at a lower cost was the combined application of prevention, continuous vaccination and treatment. But in the absence of this, the alternative measure that offer similar or same result is the combined application of screening, prevention and vaccination. These findings were affirmed and aligned with policy intervention measures for MVD as stated in the work of [2].

6 Conclusion

In this paper, a mathematical model was developed and analysis was performed on the transmission dynamics of MVD with optimal control and cost-effectiveness analysis based on lesson from EVD. The basic reproduction number was computed, which plays the role of a threshold value for the dynamics of the system. Both reproduction numbers with and without control strategies were derived. The control reproduction number was used to determine the drastic reduction or complete eradication of MVD during the time interval when the controls are applied. The local and global stabilities of the disease-free equilibrium were derived, while the local stability and existence of a bifurcation phenomenon for the Marburg persistent steady states were also proved. The model was optimized using screening, prevention, continuous vaccination and treatment as control measures. It was deduced from the numerical results that the application of all four controls provide less effort and time to reduce MVD, while the intervention that offered the greatest effectiveness at a lower cost was the combined application of prevention, continuous vaccination and treatment. The findings obtained in this article aligned with policy intervention measures for MVD as stated in the work of [2]. Just as the work of [2], a limitation from the current article is that it considered real data from just one country and thus cannot be used to form a generalization for all countries experience MVD transmission due to several geographical and cultural characteristics. Despite this limitation, the model provides a good description of the ongoing MVD outbreak.

Acknowledgements
The authors are thankful to the handling editor and the anonymous reviewers for their constructive comments and suggestions that greatly improved the presentation of the article.

Author contributions
JAM: Conceptualization, supervision, investigation, validation, mathematical and formal analysis. NK-DOO: Mathematical analysis, investigation, validation, formal analysis, parameter estimation, optimal control, sensitivity analysis, cost effectiveness, writing original draft, writing review and editing. RNB: Investigation and validation. FOB: Formal analysis and investigation, KB: Literature review, writing original draft. V.A: formal analysis, review and editing. R.A: Investigation, writing review and validation. All authors read and approved the final manuscript.

Funding
The authors did not receive any funding for the work.

Data availability
Data included in the article could be derived from https://www.who.int/emergencies/disease-outbreak-news/item/2023-DON467.

Declarations

Competing interests
The authors declare no competing interests.

Author details
[1]Department of Computer Science, Sunyani Technical University, Sunyani, Ghana. [2]Kwame Nkrumah University of Science and Technology, Kumasi, Ghana. [3]Akenten Appiah-Menka University of Skill Training and Entrepreneurial Development, Kumasi, Ghana. [4]African Institute for Mathematical Sciences, Accra, Ghana.

Received: 9 April 2024 Accepted: 28 August 2024 Published online: 31 October 2024

References

1. Schuh, A.J., Amman, B.R., Jones, M.E., Sealy, T.K., Uebelhoer, L.S., Spengler, J.R., Martin, B.E., Coleman-McCray, J.A.D., Nichol, S.T., Towner, J.S.: Modelling filovirus maintenance in nature by experimental transmission of Marburg virus between Egyptian rousette bats. Nat. Commun. **8**(1), 14446 (2017)
2. Wirsiy, F., Nkfusai, C., Bain, L.: The spin framework to control and prevent the Marburg virus disease outbreak in equatorial Guinea. Pan Afr. Med. J. **44**, 110 (2023)
3. CDC, et al.: Outbreak of Marburg virus hemorrhagic fever – Angola, October 1, 2004-March 29. Morb. Mort. Wkly. Rep. **54**(12), 308–309 (2005)
4. Ajelli, M., Merler, S.: Transmission potential and design of adequate control measures for Marburg hemorrhagic fever. PLoS ONE **7**(12), 50948 (2012)
5. Tiraga, F.M., Kavi, L.C., Neudauer, N.A.: Comparing small world network and traditional models of Marburg virus disease. J. Math. Comput. Sci. **11**(6), 7773–7792 (2021)
6. Qian, G.Y., Edmunds, W.J., Bausch, D.G., Jombart, T.: A mathematical model of Marburg virus disease outbreaks and the potential role of vaccination in control. BMC Med. **21**(1), 439 (2023)
7. Addai, E., Adeniji, A., Ngungu, M., Tawiah, G.K., Marinda, E., Asamoah, J.K.K., Khan, M.A.: A nonlinear fractional epidemic model for the Marburg virus transmission with public health education. Sci. Rep. **13**(1), 19292 (2023)
8. Washachi, D.J., Orapine, H.O., Baidu, A.A., Amoka, J.A.: Mathematical model for the transmission dynamics of Marburg virus diseases with contact tracing and effective quarantine
9. Van den Driessche, P., Watmough, J.: Further notes on the basic reproduction number. In: Mathematical Epidemiology, pp. 159–178 (2008)
10. Castillo-Chavez, C., Song, B.: Dynamical models of tuberculosis and their applications. Math. Biosci. Eng. **1**(2), 361–404 (2004)
11. Gervas, H.E., Opoku, N.K.-D.O., Ibrahim, S., et al.: Mathematical modelling of human African trypanosomiasis using control measures. Comput. Math. Methods Med. **2018**, 5293568 (2018)
12. Opoku, N.K.-D.O., Afriyie, C.: The role of control measures and the environment in the transmission dynamics of cholera. Abstr. Appl. Anal. **2020**, 2485979 (2020)
13. Gumel, A.B.: Causes of backward bifurcations in some epidemiological models. J. Math. Anal. Appl. **395**(1), 355–365 (2012)
14. Brauer, F., Castillo-Chavez, C., Feng, Z.: Endemic disease models. In: Mathematical Models in Epidemiology, pp. 63–116. Springer, Berlin (2019)
15. Opoku, N.K.-D.O., Nyabadza, F., Gwasira, E.N.: Modelling cervical cancer due to human papillomavirus infection in the presence of vaccination. Open J. Math. Sci. **3**(1), 217–233 (2019)
16. Opoku, N.K.-D.O., Borkor, R.N., Adu, A.F., Nyarko, H.N., Doughan, A., Appiah, E.M., Yakubu, B., Mensah, I., Salifu, S.P., et al.: Modelling the transmission dynamics of meningitis among high and low-risk people in Ghana with cost-effectiveness analysis. Abstr. Appl. Anal. **2022**, 9084283 (2022)
17. Kortepeter, M.G., Dierberg, K., Shenoy, E.S., Cieslak, T.J., et al.: Marburg virus disease: a summary for clinicians. Int. J. Infect. Dis. **99**, 233–242 (2020)
18. De Figueiredo, A., Simas, C., Karafillakis, E., Paterson, P., Larson, H.J.: Mapping global trends in vaccine confidence and investigating barriers to vaccine uptake: a large-scale retrospective temporal modelling study. Lancet **396**(10255), 898–908 (2020)
19. Cuomo-Dannenburg, G., McCain, K., McCabe, R., Unwin, H.J.T., Doohan, P., Nash, R.K., Hicks, J.T., Charniga, K., Geismar, C., Lambert, B., et al.: Marburg virus disease outbreaks, mathematical models, and disease parameters: a systematic review. Lancet Infect. Dis. **24**(5), E307–E317 (2023)

Publisher's Note